Received January 20, 2019, accepted February 11, 2019, date of publication February 28, 2019, date of current version March 8, 2019.

Digital Object Identifier 10.1109/ACCESS.2019.2900047

Variable Universe Fuzzy Logic-Based Hybrid LFC Control With Real-Time Implementation

SADDAM AZIZ[1], (Student Member, IEEE), HUAIZHI WANG[2], (Member, IEEE), YITAO LIU[2], (Member, IEEE), JIANCHUN PENG[2], (Senior Member, IEEE), AND HUI JIANG[1]

[1]College of Optoelectronic Engineering, Shenzhen University, Shenzhen 518060, China
[2]College of Mechatronics and Control Engineering, Shenzhen University, Shenzhen 518060, China

Corresponding author: Huaizhi Wang (wanghz@szu.edu.cn)

This work was supported in part by the National Natural Science Foundations of China under Grant 51707123, in part by the Natural Science Foundations of Guangdong Province Under Grant 2017A030310061, Grant 2016A030313041, and Grant 2017A030310317, and in part by the Foundation of Shenzhen Science and Technology Committee Under Grant JCYJ20170817100322198 and Grant JCYJ20170302153607971.

ABSTRACT Load frequency control (LFC) is playing an indispensable role to achieve the secure and economic operation of power grids. However, the existing LFC schemes either may rely on a nonlinear grid model under perfect operating condition with nominal parameters, or they may adopt a complicated control structure of high order. These LFC schemes may have poor control performance or even loss of stability in real-time implementation due to the grid uncertainties and the change of system operation scenarios. Consequently, a hybrid control method with two control loops considering various practical scenarios is originally proposed in this paper. In the inner loop, variable universe fuzzy logic control is applied to mitigate the impact of load disturbances on control performance. In the outer loop, an incremental genetic algorithm is employed to online optimize the control parameters. The performance of the proposed control method is comprehensively tested on a MATLAB/Simulink-based LFC model and a real-time digital simulator-based real-life 49-bus power system. The extensive results show that the proposed hybrid method exhibits comparatively better control performance than an adaptive fuzzy logic controller and an improved proportion integration controller.

INDEX TERMS Load-frequency control, variable universe fuzzy logic control, incremental genetic algorithm, real-time digital simulator.

NOMENCLATURE

A_i	State matrix in state space model
A_{xi}, B_{xi}	Fuzzy partitions on x_1 and x_2
B_{1i}	Disturbance matrix in state space model
B_{2i}	Input matrix in state space model
C_{yi}	Output matrix in state space model
D_i	Load damping parameter of the ith area
E_i	Initial universe of VFLC input variables
$F(\cdot)$	A function that identifies the structure of controller.
H_i	Inertia parameter of the ith control area
K_I, β_0	Control parameters for output contraction-expansion factor
$M_{in}(s)$	Transfer function of the nth governor-turbine in ith area
R_n	Speed regulation of the nth generator
T_{tni}	Time constant of the transfer function of governor n
T_{gni}	Time constant of the transfer function of generator n
T_{ij}	Tie-line synchronizing coefficient between two areas
U	Initial universe of VFLC output variable
X	A fuzzy set
Y_{CFIS}	Final output of conventional fuzzy inference system
Y_{VFLC}	Final output of VFLC
Y_{rt}	Real time output of all generators in ith control area
c	Center of a Gaussian membership function
$dACE$	Derivative of the area control error
f	Fitness function
m	Number of fuzzy rules
p_1, p_2	Positive constants for determining $\beta(x_1, x_2)$

The associate editor coordinating the review of this manuscript and approving it for publication was Mustafa Servet Kiran.

pf_{in}	Participating factor of the nth generator in ith area
$u_i(k)$	Reference signal of the i-th area at k-th time step
w_{2i}	External disturbance of the area i
x_i	State variables in control area i
x_{gi}	Output vector of the generators in area i
x_{ti}	Output vector of the governors in area i
x_{gni}	Output of the nth generator in area i
x_{tni}	Output of the nth governors in area i
y	Output variable of VFLC
y_i	The i-th consequence of the fuzzy rules
$y_i(k)$	VFLC output signal of the i-th area at k-th time step
$\alpha_i(x_i)$	Contraction-expansion factors of VFLC input variables
$\beta(x_1, x_2)$	Contraction-expansion factor of VFLC output variable
β_i	Frequency bias of the ith area
δ	Width of a Gaussian membership function
ε, τ	Parameters for input contraction-expansion factor
λ	Scaling factor in fitness function
$\mu_{A_{ij}}$	Activation degree of the combination of A_i and B_j
μ_X	Activation degree of the fuzzy set X
ϕ_j	Firing strength of the j-th rule
$\phi' j$	Normalized firing strength
ΔP_{Li}	Non-frequency- sensitive load change
Δf_i	Frequency deviation of the ith area
ΔP_{tie-i}	Tie lie power flow of the ith area
ΔL_{thd}	The threshold for load disturbance detection

I. INTRODUCTION

Nowadays, rapid expansion of physical grid size and publicity of increasing renewables, electric vehicles and other emerging technologies result in a complexity in power system. In this kind of complex power system, an essential role for restoring the system frequency and minimizing power flow deviations over network interchanges for each control authority is played by load frequency control (LFC) [1] if any disturbances occur, for instance, short circuit faults, plant or transmission line outages. So far, various advanced control theories and intelligent methods have been applied to develop robust and optimal LFC schemes, such as predictive control [2]–[4], robust control [5]–[7] and decentralized control [8]–[10]. Most recently, reinforcement learning based Q(λ) [11] and CEQ(λ) [12] algorithms were implemented to build two relaxed LFC control methodologies for thermal-dominated power systems.

Up to date, the LFC schemes under ideal operation condition with nominal network parameters have been extensively studied. In [13], a planar cloud based PI method was designed for LFC control to regulate the frequency deviation in interconnected power system with renewable energy. In [14], artificial sheep algorithm was implemented in a pumped hydropower energy storage to optimize the LFC parameters and thus maintain the frequency stability in an islanded microgrid. The frequency regulation performance under cyber-attack was analyzed in [15] and a novel detection countermeasure based on fluctuation threshold was developed accordingly. However, practical tests in China Southern Power Grid (CSG) reported that the LFC scheme designed under ideal operating conditions may rarely fulfill satisfactory performance if system steps into off-normal conditions [16]–[18] and sometimes loss of load or generator tripping can even face the frequency stability problem [19]. This issue has become ever challenging in recent years because of the booming penetration of renewable energy source, the changing grid topology and rapid deployment of new smart grid applications. In addition, the validation of the existing advanced LFC schemes were commonly performed on off-line simulations [6]. Apparently, this is inadequate to identify, analyze and correct any potential upcoming problems before application in a real power system [20], [21]. Therefore, the LFC scheme not only should be validated over a wide range of operating conditions so as to guarantee an optimal performance, but also should be tested and benchmarked via more specific and accurate online implementation if possible.

Recently, a self-turning control method, termed as variable universe fuzzy logic control (VFLC), is proposed. In this method, the input and output universes of discourse can be adjusted properly according to the external operating conditions [22], [23]. Various simulations and trajectory-tracking systems show that VFLC exhibits a high stability, effectiveness and efficiency [24]. In addition, VFLC is very fit for real-time hardware implementation because less memory is required and computing complexity is reduced. Nevertheless, as demonstrated in [24], the classical VFLC method is not sensitive to system uncertainties, such as network parameter perturbation and change of operating conditions, which would degrade the control performance. In other words, this method designed for a specific operating condition may be not suitable for control of another operating condition.

Recognizing the limitations of classical VFLC, a hybrid intelligent control framework based on VFLC and incremental genetic algorithm (IGA) is developed in this paper to achieve optimal LFC control over a wide range of operating conditions. Compared with similar studies, our contributions are threefold. First, we propose a new adaptive LFC control framework with two control loops based on VFLC and IGA. VFLC is applied in the inner loop to mitigate the impact of load disturbance on LFC control performance. The domains of discourse of input and output signals are automatically self-tuned according to the input variables. IGA is implemented in the outer loop to online optimize the VFLC control parameters as long as a disturbance happens and operating condition changes. Second, we define four operating conditions, including heavy load in wet season (WH), heavy load

in dry season (WL), low load in wet season (DH) and low load in dry season (DL). These four operating conditions are really existed in real life's power system. However, the impact of operating conditions on frequency regulation performance have not been analyzed in the existing LFC schemes. Therefore, we use the four operating states to test the overall performance of the proposed control framework. Third, our control framework has been validated on a real simplified 49-bus power system in real-time digital simulator (RTDS). It has been demonstrated that the proposed control framework exhibits strong adaptiveness and robustness over a wide range of operating conditions. Online real-time tests help us to disclose many potential issues that cannot be found in off-line simulations [25]. The above three points account for the major contributions of the paper.

The rest of this paper is organized as follows: Section II introduces the theory of variable universe fuzzy logic. The proposed hybrid LFC control framework is presented in Section III. We define the nominal power system operating states in Section IV. The case studies are given in Section V and conclusions are addressed in Section VI.

II. VARIABLE UNIVERSE FUZZY LOGIC

In this section, the concept of variable universe is first presented. We then introduce the inference mechanism in variable universe fuzzy logic.

A. CONCEPT OF VARIABLE UNIVERSE

Variable universe indicates that the domain of discourse of the input and output signal gradually changes along with the varying of the input variables. Assuming $X_i = [-E_i, E_i]$ $(i = 1, 2)$, $Y = [-U, U]$ are the initial universes of input variables x_1, x_2 and output variable y in VFLC, respectively. The universe can then be contracted and expanded according to the contraction-expansion factors $\alpha_i(x_i)$ and $\beta(x_1, x_2)$, mathematically described as follows,

$$X_i(x_i) = [-\alpha_i(x_i) E_i, \alpha_i(x_i) E_i] \quad (1)$$

$$Y(x_1, x_2) = [-\beta(x_1, x_2) U, \beta(x_1, x_2) U] \quad (2)$$

where $0 < \alpha \leq 1$, and $\beta > 0$.

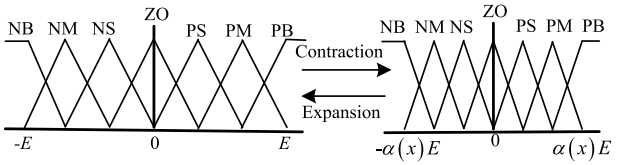

FIGURE 1. Illustration of the variable universe.

The concept of variable universe is illustrated in Fig.1. As shown, the universe with seven fuzzy partitions can be contracted and expanded to a smaller or larger universe. Each partition is a fuzzy set with triangle membership function (MF). The seven fuzzy sets are termed as NB (negative big), NM (negative medium), NS (negative small), ZO (zero), PS (positive small), PM (positive medium) and PB (positive big). The contraction and expansion processes make the variable universe preferable in real time control because contracted universe is capable for improving the control precision and expanded universe can speed up the system dynamic response [26].

B. VARIABLE UNIVERSE FUZZY INFERENCE SYSTEM

Conventional fuzzy inference system (CFIS) defines a set of rules, each of which infers fuzzy consequent given the evidence of fuzzy antecedent. In general, the rules in a zero-order Sugeno fuzzy model can be described as follows:

$$\text{If } x_1 \text{ is } A_{xi} \text{ and } x_2 \text{ is } B_{xi}, \quad \text{then } y = y_i, i = 1, 2, \ldots, m. \quad (3)$$

where $A_{xi} = \{A_{ij}\}$ $(1 \leq j \leq m)$ is the fuzzy partitions on x_1, and B_i is the partition on x_2 in the antecedent.

Then, the matching degree can be estimated by using T-norm to activate the corresponding rules as long as the crisp input vector $x = [x_1, x_2]$ is available, as follows:

$$\varphi_j(x) = \prod_{i=1}^{n} \mu_{A_{ij}}(x_i) \quad (4)$$

The firing strength of each rule is therefore normalized, as the ratio of the firing strength to the sum of all rules' firing strengths, as follows,

$$\varphi'_j(x) = \varphi_j(x) \Big/ \sum_{i=1}^{m} \varphi_i(x) \quad (5)$$

Finally, we calculate the output of each activated rule and sum them up by using a typical defuzzification method, termed as center-of-gravity. This process is mathematically represented as the following piecewise interpolation function,

$$Y_{CFIS}(x_1, x_2) = \sum_{i=1}^{m} \varphi'_i y_i \Big/ \sum_{i=1}^{m} \varphi'_i \quad (6)$$

The VFLC method is proposed by introducing a contraction-expansion factor to each input and output variable. All the contraction-expansion factors are real-time tuned based on given adaptive laws. Consequently, the final output of VFLC can be summarized as:

$$Y_{VFLC}(x_1, x_2) = \beta(x_1, x_2) Y_{CFIS}\left(\frac{x_1}{\alpha_1(x_1)}, \frac{x_2}{\alpha_2(x_2)}\right) \quad (7)$$

The factors α and β are crucial for VFLC stable operation and can be properly designed as follows [22]–[24],

$$\alpha(x) = \varepsilon + \left(|x|/E\right)^{\tau} \quad (8)$$

$$\beta(x_1, x_2) = \left| K_I \int_0^t (p_1 x_1(t) + p_2 x_2(t))\, dt + \beta_0 \right| \quad (9)$$

where p_1 and p_2 are used to convert the input vector into a scalar value. These two constants can be calculated based on Lyapunov principles in order to guarantee a high stability of the system [23]. K_I and β_0 determine the control range of VFLC.

The design of output contraction-expansion factor comes from the integral tuning idea, which describes that the change rate of β should be proportional to the control error. Therefore, the input and output contraction-expansion factors enable VFLC to exhibit with adaptive characteristics and thus the static errors can be eliminated, greatly improving the control performance of VFLC [22], [24].

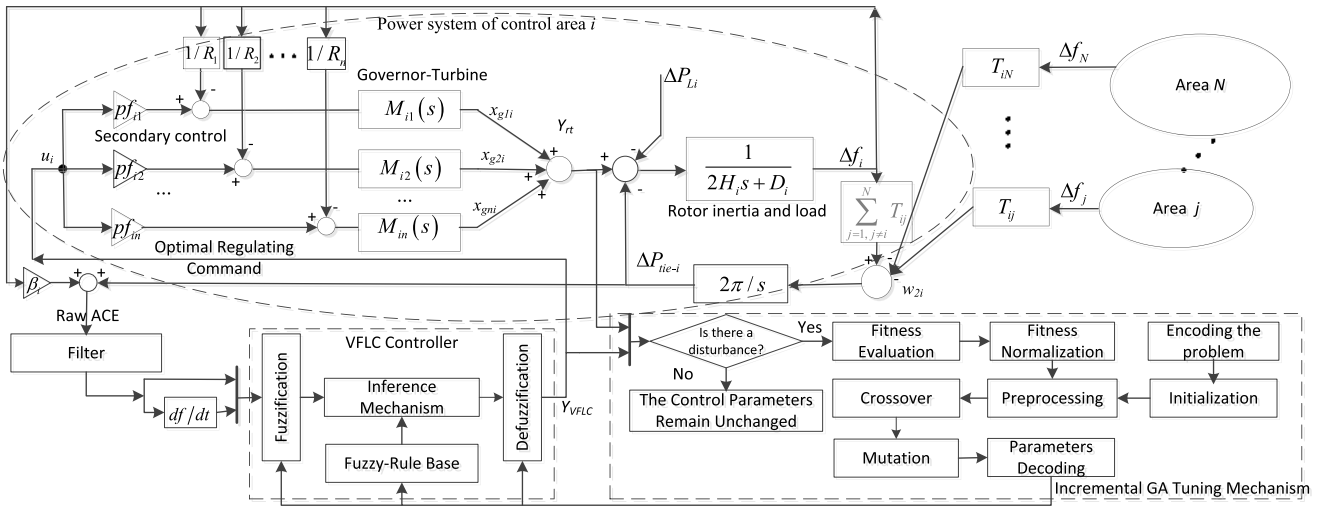

FIGURE 2. Genetic VFLC based control framework for LFC.

III. HYBRID LFC CONTROLLER CONSTRUCTION

In this Section, A new intelligent LFC control methodology is proposed. We first present the overall control framework. The details of power system model, VFLC and incremental genetic algorithm are given latter in the following subsections.

A. PROPOSED HYBRID CONTROL FRAMEWORK

The proposed intelligent LFC framework is illustrated in Fig.2. It consists of the interconnected multi-area power system model, VFLC controller and IGA tuning mechanism. The multi-area power system model describes the mathematical models of the speed governor, turbine and power networks. In load frequency control, it is assumed that all generators in each control area are synchronous and coherent [27]. This model has been widely used in the literature [3], [28]. The VFLC controller provides the optimal regulating command for frequency recovery when disturbance occurs. It consists of fuzzification, fuzzy rule base, inference mechanism and defuzzification. The IGA algorithm is implemented to real-time tune the parameters in VFLC controller.

The proposed control methodology first determines whether there has a disturbance or not in the system. Specifically, a load disturbance happens when the difference between the regulating reference Y_{VFLC} and the real-time output Y_{rt} of all generators is larger than a preset detection threshold, described as follows:

$$|Y_{VFLC} - Y_{rt}| \geq \Delta L_{thd} \tag{10}$$

If there has no disturbance in the system, the VFLC control parameters remain unchanged. Otherwise, IGA will be used to optimize the VFLC parameters. The optimization process consists of encoding, fitness evaluation, fitness normalization, preprocessing, crossover, mutation and decoding. The individual with the best performance, i.e., the minimal fitness value, is chosen as the one for decoding. Finally, the VFLC controller can be implemented for frequency regulation when their parameters have been determined. The inputs of the VFLC controller include the area control error (ACE) and its derivative *dACE*. ACE is the instantaneous difference between actual and scheduled electrical generation within a control area, taking frequency bias into consideration. It should be noted that ACE is defined within a control area. In general, the control area is naturally formed according to the administrative divisions. In China, each province actually represents an independent control area. The output signal is the reference for optimal frequency regulating. The speed governors and turbines adjust their outputs by following the reference signals, thus improving the frequency quality of the system.

B. POWER SYSTEM MODEL

In this paper, a typical power system model for load frequency control is considered. This model contains a number of interconnected control areas. The block diagram of the ith control area with n generators in an N control area power system is shown in Fig.2. The speed governor, turbine and power system, including rotating mass and load units, are described as three first-order transfer functions. In addition, the practical constraints on generation rate and the impacts of areas interface have been properly considered. Consequently, the state-space model for area i is given as below [29]:

$$\dot{x}_i = A_i x_i + B_{1i} w_i + B_{2i} u_i \tag{11}$$

$$y_i = C_{yi} x_i \tag{12}$$

where

$$x_i = \begin{bmatrix} \Delta f_i & \Delta P_{tie-i} & x_{ti} & x_{gi} \end{bmatrix}^T \tag{13}$$

$$x_{ti} = \begin{bmatrix} \Delta x_{t1i} & \Delta x_{t2i} & \dots & \Delta x_{tni} \end{bmatrix} \tag{14}$$

$$x_{gi} = \begin{bmatrix} \Delta x_{g1i} & \Delta x_{g2i} & \dots & \Delta x_{gni} \end{bmatrix} \tag{15}$$

$$u_i = F\,(ACE) \tag{16}$$

$$y_i = \beta \Delta f_i + \Delta P_{tie-i} \tag{17}$$

$$w_i = \begin{bmatrix} \Delta P_{Li} & w_{2i} \end{bmatrix} \tag{18}$$

In above equations, A_i, B_{1i} and B_{2i} represent the parameter matrices in state space model. They have the following form:

$$A_i = \begin{bmatrix} A_{i11} & A_{i12} & A_{i13} \\ A_{i21} & A_{i22} & A_{i23} \\ A_{i31} & A_{i32} & A_{i33} \end{bmatrix} \tag{19}$$

$$B_{1i} = \begin{bmatrix} B_{1i1} & B_{1i2} & B_{1i3} \end{bmatrix}^T \tag{20}$$

$$B_{2i} = \begin{bmatrix} B_{2i1} & B_{2i2} & B_{2i3} \end{bmatrix}^T \tag{21}$$

$$A_{i11} = \begin{bmatrix} -D_i/H_i & -1/H_i \\ 2\pi \sum_{j=1, j\neq i}^{N} T_{ij} & 0 \end{bmatrix} \tag{22}$$

$$A_{i12} = \begin{bmatrix} 1/H_i & \dots & 1/H_i \\ 0 & \dots & 0 \end{bmatrix}_{2\times n} \tag{23}$$

$$A_{i13} = A_{i21}^T = 0_{2\times n}; A_{i32} = 0_{n\times n} \tag{24}$$

$$A_{i22} = -A_{i23} = diag\begin{bmatrix} -1/T_{t1i} & \dots & -1/T_{tni} \end{bmatrix} \tag{25}$$

$$A_{i31} = \begin{bmatrix} -1/(T_{g1i}R_1) & \dots & -1/(T_{gni}R_n) \\ 0 & \dots & 0 \end{bmatrix}^T \tag{26}$$

$$A_{i33} = diag\begin{bmatrix} -1/T_{g1i} & \dots & -1/T_{gni} \end{bmatrix} \tag{27}$$

$$B_{1i1} = \begin{bmatrix} 1/H_i & 0 \\ 0 & -2\pi \end{bmatrix} \tag{28}$$

$$B_{1i2} = B_{1i3} = 0_{n\times 2}; \quad B_{2i1} = 0_{2\times 1}; \; B_{2i2} = 0_{n\times 1} \tag{29}$$

$$B_{2i3}^T = \begin{bmatrix} pf_{i1}/T_{g1i} & \dots & pf_{in}/T_{gni} \end{bmatrix} \tag{30}$$

where A_{i11}, A_{i12}, A_{i13}, A_{i21}, A_{i22}, A_{i23}, A_{i31}, A_{i32}, A_{i33}, B_{1i1}, B_{1i2}, B_{1i3}, and B_{2i1}, B_{2i2}, B_{2i3} are the parameter submatrices of state, disturbance and input matrices, respectively.

In this paper, we consider the LFC model (11)-(30) as the benchmark system for the design of the LFC controller. It is widely accepted in a restructured electric industry. Any power system in real world can be transformed into the LFC model (11)-(30) for automatic frequency control.

C. VFLC SYNTHESIS REALIZATION

In VFLC, there are four basic blocks, fuzzification, knowledge base, inference mechanism and defuzzification. The fuzzification block converts the crisp input into several linguistic variables for each fuzzy set using Symmetric Gaussian membership functions (MFs). Consequently, the result of each fuzzy IF-THEN rule in knowledge base is determined by using the inference mechanism. The knowledge base is actually a lookup table, which is established beforehand using our experiences. Finally, the outcomes of each fuzzy rules aggregated and converted into a crisp output through centroid defuzzification method. The principles of the four basic blocks are elaborated as below.

1) FUZZIFICATION

This block transforms every crisp input into an activation degree of each fuzzy set. At first, the input variables should be contracted or expanded according to the contraction-expansion factors, as shown in (7). Then, the activation degree of each MF can be created according to a symmetric Gaussian profile, as follows:

$$\mu_X(x_i) = e^{-0.5(x_i - c/\delta)^2} \tag{31}$$

Seven fuzzy sets have been designed for ACE, and five fuzzy sets for dACE. The ACE fuzzy sets are determined as negative big (NB), negative medium (NM), negative small (NS), zero (ZO), positive small (PS), positive medium (PM) and positive big (PB), and initialized with equal space and adequate overlap between two fuzzy sets. Obviously, six parameters, i.e., c for NM, NS, and δ for NB, NM, NS and ZO, are required to be determined beforehand because the MFs are symmetric. The dACE fuzzy sets contain NB, NS, ZO, PS and PB, and four parameters, including c for NS and δ for NB, NS and ZO, are needed to be determined beforehand. Therefore, according to (31), the ACE input variable has seven activation degrees, each of which corresponds to a membership function in a fuzzy set. The dACE input variable has five activation degrees.

2) KNOWLEDGE BASE

Knowledge base is the core part of the VFLC controller. In this paper, we design a knowledge base having 35 fuzzy rules, as shown in Table 1. Each fuzzy rule can be described in the form of IF-THEN statement, for example,

TABLE 1. Knowledge base in VFLC controller.

		dACE				
		NB	NS	ZO	PS	PB
ACE	NB	PB	PM	PM	PS	ZO
	NM	PB	PM	PS	PS	NS
	NS	PM	PS	PS	ZO	NS
	ZO	PM	PS	ZO	NS	NM
	PS	PS	ZO	NS	NS	NM
	PM	PS	NS	NS	NM	NB
	PB	ZO	NS	NM	NM	NB

If *ACE* is PB AND *dACE* is PB, then *output* is NB.

The precursor of these rules includes two parts, i.e., ACE and dACE. Both of them are combined with *AND* operator. In the rule, AND is an operator which means a multiplication symbol.

3) INFERENCE MECHANISM

This subsection aims to produce the output of each fuzzy rule. It is achieved by using (4)-(5). Simply speaking, the matching degree of each IF-THEN rule is taken as the output of the rule. The output of each rule is then normalized as the ratio of the matching degree of the rule to the sum of all rule outputs. Consequently, there are 35 outputs in inference mechanism. Therefore, a defuzzification process is required to transform the outputs of all rules into a crisp output.

4) DEFUZZIFICATION

The goal of the defuzzification is to get a continuous variable from all the outputs of fuzzy rules. This would be easy if the rule output values were exactly those obtained from fuzzification of a given input. However, all rule output values are calculated independently, in most cases they do not represent such a set of input numbers. In this paper, we use a centroid defuzzification method to map the rule outputs into a crisp value, as shown in (6)-(9). A common algorithm is: (a) take the contracted/expanded inputs into (6) to calculate a centroid value; (b) estimate the output contraction-expansion factor according to (9); (c) we then can obtain the final crisp output based on (7). The obtained crisp output is exactly the optimal command for real-time frequency regulation.

D. OPTIMAL PARAMETERS TUNING

Apparently, the control performance of VFLC controller relies on the MF parameters and variable universe design parameters. MF parameters contain three center parameters and seven width parameters of the Gaussian membership functions, as presented in III-C. Design parameters include ε, τ, K_I, and β_0 of the contraction-expansion factors. In principle, the ten VFLC parameters are determined beforehand according to the experience. However, a set of parameters that are optimal in a certain operating condition may not suitable for the control of another operating condition. In other words, the VFLC controller lacks adaptiveness over multiple operating conditions of power systems. Therefore, incremental genetic algorithm (IGA) [30] is introduced and designed for online optimization of the parameters in VFLC.

IGA originates from the classical genetic algorithm (GA), which is a famous heuristic search algorithm [31]. It mimics natural population reproduction and selection operations to achieve robust and efficient optimization [32], [33]. The differences between IGA and classical GA are twofold. The first is that IGA updates only one individual at each generation to improve the calculation efficiency. The other is that IGA starts with an initial population that contains various chromosomes saved from the classical GA run for the initial problem version. These chromosomes are best feasible and best infeasible chromosomes so as to ensure sufficient diversity within them. IGA consists of problem encoding, fitness evaluation and normalization, preprocessing, crossover, mutation and problem decoding, as given below.

1) PROBLEM DECODING

The parameters required to be optimized in VFLC controller are represented as a set of artificial chromosomes that IGA can handle. Every chromosome corresponds to a parameter. A set of chromosomes is actually a solution, termed as an individual, to the optimization problem. Afterwards, twenty individuals are randomly generated, allowing the entire range of possible solutions.

2) FITNESS EVALUATION AND NORMALIZATION

The intelligent LFC control framework is proposed based on VFLC and IGA for optimal control. The control performance can be assessed using certain criteria, such as integral of absolute error, integral of square error and integral of time multiplied absolute error. However, the studies in [11] and [12] show that it is essential to integrate a penalty of excessive control into the fitness evaluation function in order to reduce the wear and tear of generators. Therefore, we use an index termed as integral of absolute control rate and error (IACRE) to evaluate the performance of an individual, as follows,

$$f_i = \int_0^T \left(|u_i(k) - y_i(k)| + \lambda\,|u_i(k) - u_i(k-1)|\right) dt \qquad (32)$$

The performance of all individuals from problem decoding can be estimated based on (32), resulting in a fitness value. We then normalize the fitness values of all individuals.

3) PREPROCESSING

This process aims to select two individuals to undergo crossover and mutation. Roulette wheel selection technique is used for selecting potentially useful individuals. This technique is detailed in [34].

4) CROSSOVER AND MUTATION

IGA performs natural operators such as crossover and mutation to produce a new chromosome. Crossover operator is used to generate one-child individual by combining the information extracted from selected parents in preprocessing. The newborn individual replaces the chromosome with the worst fitness value. Mutation operator is then applied as a random search process to overcome irrecoverable optimality [35].

5) PROBLEM DECODING

Then, the chromosome with the highest fitness value is decoded. A set of parameters is then obtained. These parameters is exactly the control parameters in VFLC.

The above presentations constitute the main steps of the IGA applied to optimize the parameters in VFLC. In real time application, only one chromosome is evaluated at every time step by using the fitness function (32). The obtained fitness value indicates the variation tendency of the fitness of each chromosome to the target. Two chromosomes are then selected in preprocessing. Crossover and mutation are applied to generate a new children individual and the one with worst performance is deleted. Finally, the one with the best control performance is decoded into the solution space and used for real-time parameter optimizations of VFLC. The flowchart of the algorithm is detailed in Fig.2.

IV. NOMINAL OPERATION STATES FOR POWER SYSTEM

Power system operating states are continuously changing over a wide range because of varying loads and renewable generations, which are largely influenced by e.g. seasonal

and daily factors. Heavy load level requires more generation units. Hence, the system inertia, damping coefficient and AGC participating factors have been affected. In addition, the behaviors of generating units equipped with AGC functions have also an impact on LFC control process. The typical time delay in the secondary frequency regulation of thermal units ranges from 0.5-2 minutes because the turbine-boiler system has lager time constant to respond. In contrast, hydro or gas units follow the reference signal with a far less time delay. Consequently, more hydro units are required to participate in frequency regulation in wet season than that in dry season because of the sufficient reservoir and the fast response of the hydro generators. Therefore, the classification of operating states is more difficult when considering the changing grid structure, generator type, the increasing size of modern power system. Conventional LFC control method designed based on one or several specific operating states may be not suitable anymore for today's power system.

Generally, power system nominal operating states can be classified according to the load level and seasonal condition in order to simplify the dynamic analysis involved in LFC controller. Take China Southern Power Grid (CSG) for example, four typical operating states: heavy load in wet season (WH) and dry season (WL), low load in wet season (DH) and dry season (DL), are categorized [36]. In each operating state, an improved PI controller is developed to eliminate the frequency bias. However, the improved PI controller neglects the participating factors in generating units, system parameter uncertainties, and load dynamic characteristics. Previous experiments performed in the dispatch centers of CSG show that the resultant controller may hardly provide a satisfactory performance over all operating states, and sometimes even jeopardize the system stability due to the PI parameters toggling [37]. Moreover, many existing LFC schemes adopt a high-order controller, which limits its practical value for real-time implementation [6], [37]. To overcome the above inefficiencies, this paper proposes a new hybrid intelligent LFC control framework based on VFLC and IGA to fulfill control objective over multiple operating states of power system.

V. CASE STUDIES

The proposed hybrid control framework has been validated on a three-area LFC model and a five-area power system model on real time digital simulator (RTDS).

A. THE THREE-AREA LFC MODEL

1) MODEL DESCRIPTION

The proposed hybrid LFC scheme is firstly evaluated on a three-area LFC model established using Matlab/Simulink. The Simulink model of each LFC area is the same as shown in Fig.2. The overall topology of the three area model is given in [37]. To simplify the analysis, the proposed scheme is only applied to area 1, whereas the other two areas adopt the traditional control method based on improved PI. Four groups of parameters are carefully selected for four kinds of operating states. The generator installation capacities in area 1 are 700MW, including 55% of thermal units, 20% of hydro plants, 10% of gas power and 15% of renewable generation. The LFC participating factors differ a lot in four operating states because the power generation of renewable generators varies significantly over the four seasons. The system parameters in area 1 are partly listed in Table 2.

TABLE 2. Part of the parameters in area 1.

	D	$2H$	B	T_{12}	T_{13}	Load
WH	0.015	0.1667	12.6225	0.2	0.4	562
WL	0.0107	0.1405	10.5141	0.15	0.35	349
DH	0.013	0.1524	11.1259	0.15	0.3	415
DL	0.009	0.1347	9.0521	0.1	0.2	283

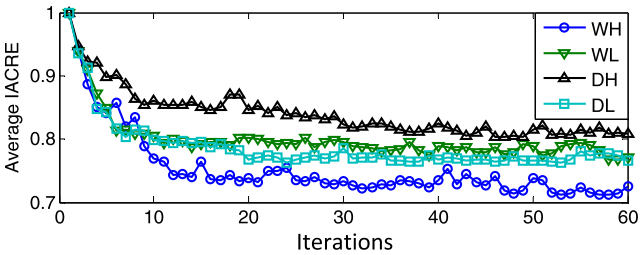

FIGURE 3. The converging curve of the average of IACRE.

TABLE 3. Final MF parameters of ACE input under four nominal states.

	C_{NM}	C_{NS}	δ_{NB}	δ_{NM}	δ_{NS}	δ_{ZO}
WH	0.4663	0.8678	0.0154	0.6452	0.0303	0.1273
WL	0.4832	0.8995	0.6203	0.1007	0.6901	0.0851
DH	0.3592	0.7636	0.0170	0.0496	0.8427	0.2933
DL	0.4973	0.7901	0.0375	0.8855	0.8333	0.0446

2) CONTROLLER TRAINING

In this paper, the hybrid LFC scheme is implemented at a steady state under a given nominal operating state. A sudden load variation is then applied to area 1 and latterly removed. Afterwards, the control performance is evaluated based on (32), resulting in a set of updated VFLC parameters. Consequently, using the improved control parameters, a set of input-output pairs is generated to form the training patterns for the proposed LFC scheme. The training process continues until the preset stopping criterion is satisfied. Fig. 3 shows the converging curve of the average of IACRE per unit under four nominal operating states. It is clear that the average of IACRE has converged in about 30 iterations and final MFs indeed vary according to the initial membership functions. Note that the IACRE curves occasionally increase in some cases. This is because IGA is a heuristic algorithm whose performance may go worse when the crossover and mutation operators are performed. The control parameters under the other three operating states can be obtained in a similar manner and the final converged MF parameters are partly presented in Table 3.

3) SIMULATION RESULTS

The main objective of the simulations is to stabilize a frequency of 50Hz. The performance of the proposed hybrid LFC scheme under WH operating states is compared with an improved PI controller [38] and an adaptive fuzzy logic controller [39] (AFLC), as shown in Fig. 4. The obtained results reveal that the proposed hybrid LFC control framework is capable to keep the frequency within the limits, i.e., 0.2Hz [37], with good transient performance, even the frequency goes outside of the limit for a while. In addition, it also can be seen that the system response of the proposed method is very similar to the performance of improved PI and AFLC. This is because the control parameters of PI and AFLC are well tuned under nominal states and the degree to be optimized is very limited. Similar conclusions can also be obtained under the other three nominal operation states.

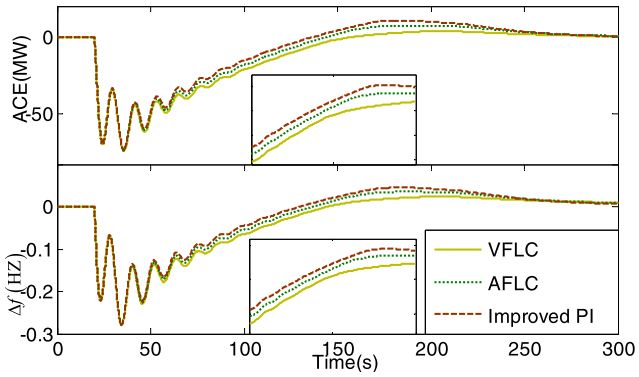

FIGURE 4. The performance of the three algorithms under WH operating state.

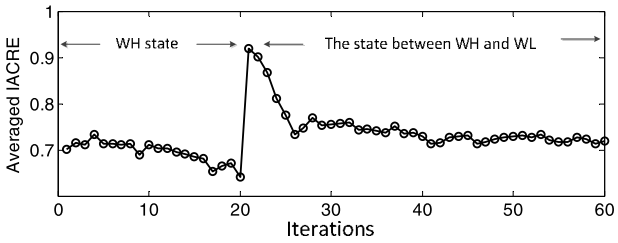

FIGURE 5. The converging curve of IACRE from WH state to the state between WH and WL.

To demonstrate the robustness of the proposed LFC scheme under an external varying environment, the simulations in which the system parameters are set to that between two nominal states, i.e., between WH and WL or between DH and DL, are carried out. Most of the daily operations are in this case due to varying load and intermittent sustainable energy. The converging curve of the IACRE varying from WH to the state between WH and WL is given in Fig. 5, showing that the IACRE index eventually converges after sufficient iterations. This means that the IACRE is transferred from a balance point to another balance point. It also can be shown that the IACRE increases a lot at the 20th iteration. This is because the LFC model parameters is switched from WH to the state between WH and WL. The performance

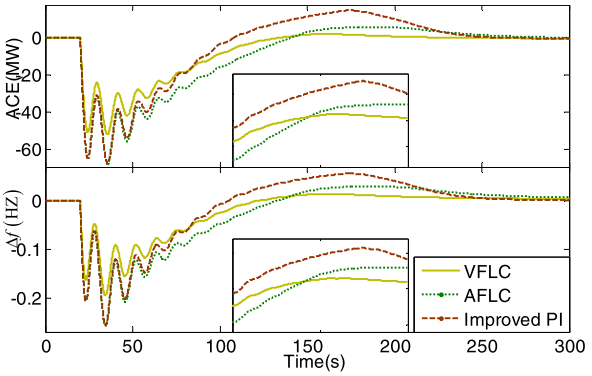

FIGURE 6. The response under the state between WH and WL.

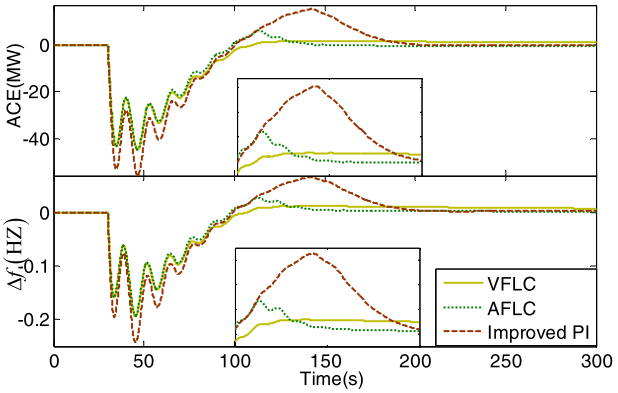

FIGURE 7. The response under the state between DH and DL.

of VFLC parameters in WH is not optimal anymore in the state between WH and WL, resulting in a large fluctuation of IACRE. Finally, the parameters of the hybrid controller are finally optimized. The learning ability of the proposed controller is examined by performance comparison analysis with improved PI and AFLC. The step responses of the three types of controller under the state between WH and WL are shown in Fig. 6, and the responses under the state between DH and DL are shown in Fig. 7. From these two figures, it is clear that the proposed hybrid controller based on VFLC exhibits lower overshoots and also has a shorter settling time. In addition, the proposed method oscillates with a smaller amplitude. On the contrary, the improved PI and AFLC oscillate sharply. Therefore, we can conclude that the proposed control framework has a superior performance with strong adaptiveness, indicating that the VFLC control parameters can be online tuned as the power system operating state changes. In addition, it also can be seen that Fig. 4 and Figs.6-7 are very similar. This is because the same step load is used to test the control performance of the three benchmark algorithms, resulting in the same oscillating patterns of ACE and frequency deviations.

In order to further investigate the effectiveness and robustness of the hybrid LFC scheme, the performance under different operating states and disturbance levels were studied [40]. Here, 20 groups of system parameters were carefully selected to represent twenty operating states and the performance

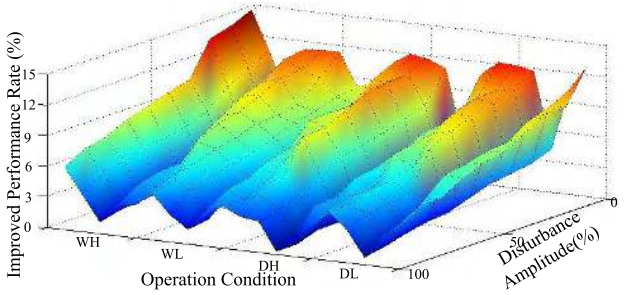

FIGURE 8. The improved performance rate of the proposed scheme over PI.

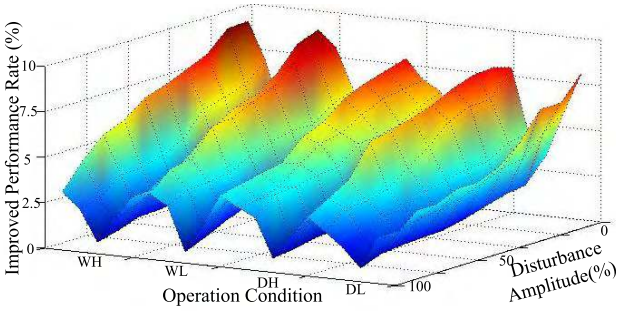

FIGURE 9. The improved performance rate of the hybrid LFC scheme over AFLC.

under each operating state was tested by using the proposed hybrid control framework, improved PI and AFLC. The amplitude of the disturbance level is assumed to range from 0% to 100% of the maximum. This range was considered to appropriately cover the range of possible disturbances. That is, a disturbance amplitude and an operating state correspond to a unique position in the disturbance/operating state (D/O) space. By testing the performance of all positions in the D/O space, the distribution of the improved performance rate can be systematically estimated. The improved performance rate is calculated as the ratio of IACRE difference between the proposed control method and AFLC/improved PI to the IACRE of AFLC/improved PI. Such that, a comprehensive overview on the performance quality and the robustness of the proposed LFC scheme can be obtained. The comparative results are shown in Fig. 8 and Fig. 9 respectively. It is obvious that the performance using the proposed control framework are superior to that of improved PI and AFLC in all positions, implying that the proposed control framework exhibits strong adaptiveness, high efficiency and robustness over multiple operating states.

B. REAL-TIME LABORATORY SIMULATION

A large scale RTDS system for power system research was installed at the Power System Simulation Department, Electric Power Research Institute (EPRI), China Southern Power Grid (CSG), as shown in Fig. 10. It contains 35 RTDS racks, and lots of periphery hardware and software equipment, such as relays and secondary frequency control system, on which the whole CSG transmission network has been established.

FIGURE 10. RTDS system in EHV power transmission company, CSG.

The RTDS provides an applicable platform to test the overall performance of the proposed hybrid intelligent LFC scheme based on VFLC and IGA.

1) RTDS DESCRIPTION

As a real-time digital simulator, RTDS is capable for the design, development and test of power system protection and control schemes. The proposed hybrid intelligent scheme was programmed on a graphical user interface in RTDS termed as RSCAD, in which electromagnetic transient simulation can be performed with a typical time step of 10-80 μs. The major advantage of RTDS is its advanced parallel processing capability in modular units called rack. Each rack consists of several digital signal processors, such as Giga Processor Card and Triple processor cards. These processors are used to solve power system equations. The communications between racks or that between RTDS and workstation are transferred via Workstation Interface Card.

2) SYSTEM CONFIGURATION

The 49-bus test power system contains 12 generators, 49 transmission lines and 37 load centers. It is established by using electrical components from customized component libraries. The test system is performed on two racks and has four subareas, as shown in Fig.11. The subareas are randomly defined. The definition of the subareas will not change the performance of the proposed control framework. This is because the input variables of the proposed control framework are ACE and dACE. Both of the two variables are independent from the control areas and thus are model free. In each area, an independent LFC controller is designed accordingly. In normal state, the total generation in area C could not fully satisfy its load demand and so extra power is required to be imported in this area via tie-lines. The generator parameters in Area C are given in Table 4.

The proposed hybrid LFC methodology was built in a personal computer based on self-defined C Builder. The output of the computer program is the reference set point that

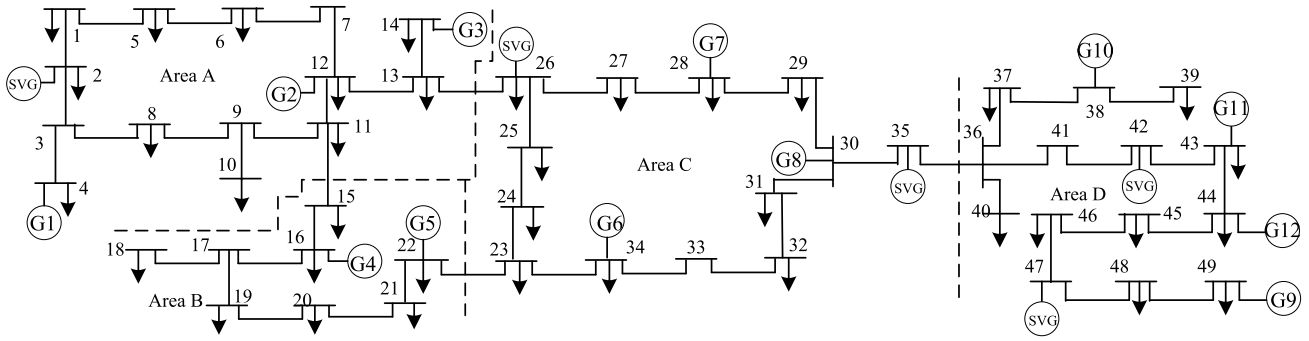

FIGURE 11. The single-line diagram of the test system.

TABLE 4. The generator parameters in area C.

Unit	Capacity (MW)	GRC (%/min)	TRT (s)	TDB (%/min)	TVTC (s)
G6	500	3	0.25	0.1	0.04
G7	600	4	0.4	0.2	0.04
G8	1100	5	0.6	0.35	0.04
GRC denotes generation rate constraint, TRT and TDB are turbine response time and dead band respectively, and TVTC denotes turbine valve time constant.					

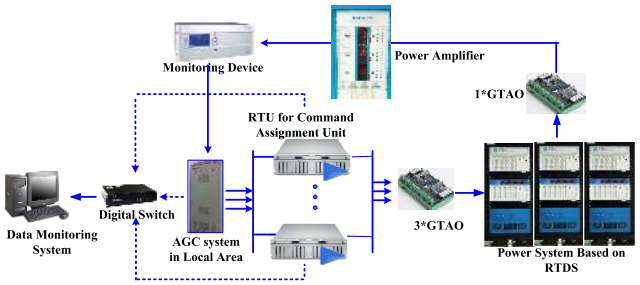

FIGURE 12. The hardware of the LFC control system.

is used to eliminate the ACE bias. This reference signal is transmitted to Remote Terminal Units (RTUs), each of which is connected to a real-time simulator via a series of GTAO devices with A/D and D/A converters. These converters act as interfaces between RTUs and real-time simulators. In addition, the system state signals, such as frequency deviation and tie-line power exchange, are monitored via monitoring devices and transferred to load frequency control system. The hardware topology of the LFC control system is shown in Fig.12.

3) COMPARATIVE SIMULATIONS

In order to demonstrate the superior performance of the proposed LFC control methodology, a load shedding scheme with 220MW is carried out under a given stochastic operating state. The participating factors of generators 6-8 are set to 0.15, 0.45, and 0.4, respectively. Improved PI and AFLC are used as the benchmarks for performance comparison. The system responses, i.e., the frequency deviation Δf, ACE, and tie-line power flow, are presented in Figs. 13-14, respectively.

Considering ACE and frequency deviations, it can be observed from Fig.13 that the settling times of the proposed

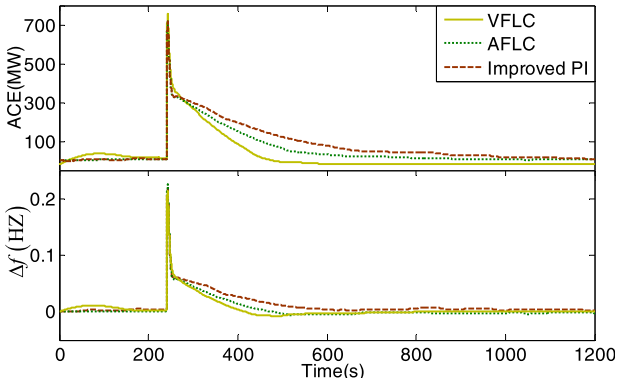

FIGURE 13. The frequency deviation and ACE.

hybrid LFC scheme, improved PI and AFLC are 510s, 1040s and 690s, respectively. It is clear that the proposed scheme based on VFLC exhibits a smaller settling time, which means the proposed scheme has a better control performance than the improved PI and AFLC. In addition, all ACEs and frequency deviations are kept within acceptable range without any fluctuations. This indicates that the proposed hybrid LFC scheme based on VFLC and IGA is stable when a load shedding happens. With respect to the tie-line power flows, it is clear from Fig.14 that the proposed LFC scheme has the fastest transient responses, i.e., shortest rise time, when compared to improved PI and AFLC. It also can be seen that the proposed LFC scheme has a stable tie-line power flows in all areas. Therefore, it can be concluded that the proposed hybrid scheme based on VFLC and IGA exhibits the best overall performance among the benchmark control systems. This is because the proposed hybrid scheme is very adaptive. Concretely, it provides a faster control when the system has a large ACE deviation, and a more accurate but slower control when the system has a small ACE deviation. This adaptiveness cannot be provided by the benchmark control systems. Therefore, the proposed AFLC based control scheme exhibits a strong learning capability, which is associated with the feedback state signal. This learning capability makes the performance attractive in real-time control over different operating states. It should be noted that the proposed methodology is used for load frequency control, which has no

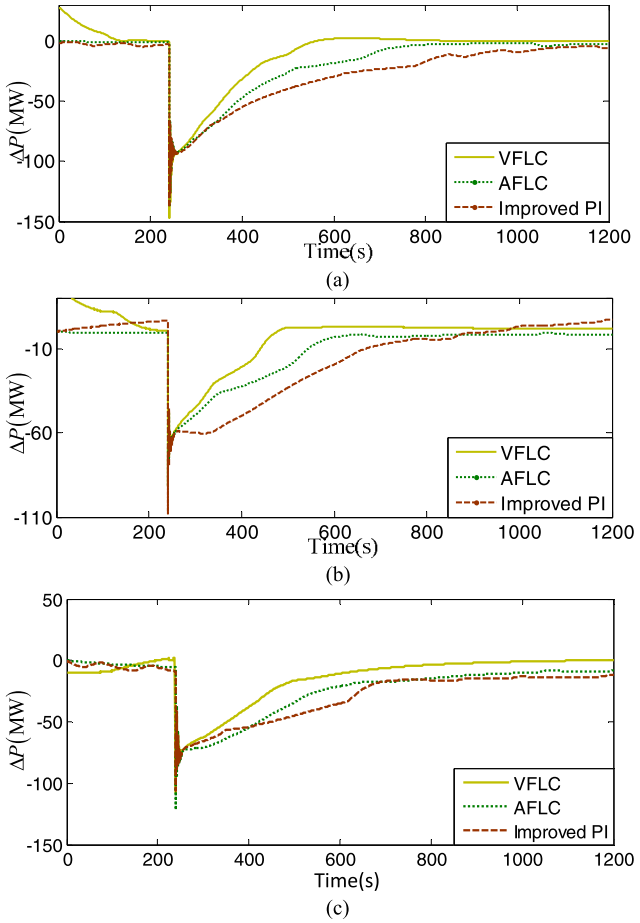

FIGURE 14. Tie-line power flows. (a) Tie-line power flows in area A. (b) Tie-line power flows in area B. (c) Tie-line power flows in area D.

TABLE 5. Comparative results of daily statistical BAAL indices.

	AREA A	AREA B	AREA C	AREA D
IMPROVED PI	90.13%	88.51%	89.06%	87.97%
AFLC	91.15%	90.47%	92.36%	89.70%
VFLC	93.51%	94.02%	94.84%	91.96%

rotor angle stability problem. In other words, all generators in LFC are coherent and synchronous because the system frequency is proportional to the difference between generations and demands [27].

In order to demonstrate the preference of the proposed scheme, the balancing authority ACE limit (BAAL) [41] is used as the index for comparison. It is recently used as a frequency control performance standard and has been applied to limit the unscheduled tie-line power flows in authorities. Accordingly, a day-to-day statistical experiment under the BAAL standard is carried out for load frequency control. The proposed LFC scheme is applied in all control areas, resulting in various BAAL indices as shown in Table 5. Obviously, the proposed VFLC methodology has the highest BAAL index, indicating that the statistical frequency deviations of the proposed methodology are lowest. This makes the proposed scheme very robust in future smart grid with high penetration of renewable powers. The better performance of the proposed scheme attributes to its learning capability and adaptiveness over a wide range of operating conditions.

VI. CONCLUSIONS

This paper proposes a novel hybrid control methodology based on VFLC and IGA for adaptive load frequency control over a wide range of operating states. This methodology consists of two control loops. The VFLC theory is applied in the inner loop to enable the robust control in all possible disturbance levels. IGA is applied in the outer loop to tune the VFLC parameters considering various operating states. The proposed scheme was tested on a three-area LFC model, in which four nominal states and sixteen off-nominal states are considered based on load and climate conditions. It has been demonstrated that the proposed scheme is capable to generate mature membership functions and fuzzy rules. In addition, extensive results show that the proposed hybrid LFC scheme exhibits competitive performance when compared to other LFC schemes, such as the improved PI and AFLC. Besides, a practical 49-bus power system in RTDS is used to validate the feasibility and efficiency of the proposed control framework. The obtained results also show that the proposed algorithm is very attractive in real-time implementations because of its satisfactory system response and better statistical BAALs.

REFERENCES

[1] N. Jaleeli, L. S. VanSlyck, D. N. Ewart, L. H. Fink, and A. G. Hoffmann, "Understanding automatic generation control," *IEEE Trans. Power Syst.*, vol. 7, no. 3, pp. 1106–1122, Aug. 1992.
[2] S. Kayalvizhi and D. M. V. Kumar, "Load frequency control of an isolated micro grid using fuzzy adaptive model predictive control," *IEEE Access*, vol. 5, pp. 16241–16251, 2017.
[3] M. Ma, C. Zhang, X. Liu, and H. Chen, "Distributed model predictive load frequency control of the multi-area power system after deregulation," *IEEE Trans. Ind. Electron.*, vol. 64, no. 6, pp. 5129–5139, Jun. 2017.
[4] A. M. Ersdal, L. Imsland, and K. Uhlen, "Model predictive load-frequency control," *IEEE Trans. Power Syst.*, vol. 31, no. 1, pp. 777–785, Jan. 2016.
[5] L. Xi *et al.*, "Smart generation control based on multi-agent reinforcement learning with the idea of the time tunnel," *Energy*, vol. 153, pp. 977–987, Jun. 2018.
[6] Ibraheem, P. Kumar, and D. P. Kothari, "Recent philosophies of automatic generation control strategies in power systems," *IEEE Trans. Power Syst.*, vol. 20, no. 1, pp. 346–357, Feb. 2005.
[7] P. Ojaghi and M. Rahmani, "LMI-based robust predictive load frequency control for power systems with communication delays," *IEEE Trans. Power Syst.*, vol. 32, no. 5, pp. 4091–4100, Sep. 2017.
[8] T. C. Yang, Z. T. Ding, and H. Yu, "Decentralised power system load frequency control beyond the limit of diagonal dominance," *Int. J. Elect. Power Energy Syst.*, vol. 24, no. 3, pp. 173–184, Mar. 2002.
[9] L. Xi, Z. Zhang, B. Yang, L. Huang, and T. Yu, "Wolf pack hunting strategy for automatic generation control of an islanding smart distribution network," *Energy Convers. Manage.*, vol. 122, pp. 10–24, Aug. 2016.
[10] A. Delavari and I. Kamwa, "Improved optimal decentralized load modulation for power system primary frequency regulation," *IEEE Trans. Power Syst.*, vol. 33, no. 1, pp. 1013–1025, Jan. 2018.
[11] T. Yu, B. Zhou, K. W. Chan, L. Chen, and B. Yang, "Stochastic optimal relaxed automatic generation control in non-Markov environment based on multi-step $Q(\lambda)$ learning," *IEEE Trans. Power Syst.*, vol. 26, no. 3, pp. 1272–1282, Aug. 2011.
[12] T. Yu, H. Z. Wang, B. Zhou, K. W. Chan, and J. Tang, "Multi-agent correlated equilibrium $Q(\lambda)$ learning for coordinated smart generation control of interconnected power grids," *IEEE Trans. Power Syst.*, vol. 30, no. 4, pp. 1669–1679, Jul. 2015.

[13] Z. Li, X. Li, and B. Cui, "Planar clouds based load frequency control in interconnected power system with renewable energy," *IEEE Access*, vol. 6, pp. 36459–36468, 2018.
[14] Y. Xu, C. Li, Z. Wang, N. Zhang, and B. Peng, "Load frequency control of a novel renewable energy integrated micro-grid containing pumped hydropower energy storage," *IEEE Access*, vol. 6, pp. 29067–29077, 2018.
[15] C. Chen, M. Cui, X. Wang, K. Zhang, and S. Yin, "An investigation of coordinated attack on load frequency control," *IEEE Access*, vol. 6, pp. 30414–30423, 2018.
[16] F. Daneshfar and H. Bevrani, "Load-frequency control: A GA-based multi-agent reinforcement learning," *IET Gener., Transmiss. Distrib.*, vol. 4, no. 1, pp. 13–26, Jan. 2010.
[17] H. Bevrani, P. R. Daneshmand, P. Babahajyani, Y. Mitani, and T. Hiyama, "Intelligent LFC concerning high penetration of wind power: Synthesis and real-time application," *IEEE Trans. Sustain. Energy*, vol. 5, no. 2, pp. 655–662, Apr. 2014.
[18] L. D. Douglas, T. A. Green, and R. A. Kramer, "New approaches to the AGC non-conforming load problem," *IEEE Trans. Power Syst.*, vol. 9, no. 2, pp. 619–628, May 1994.
[19] D. P. Kothari and I. J. Nagrath, *Modern Power System Analysis*, 3rd ed. Singapore: McGraw-Hill, 2003.
[20] S.-M. Baek and J.-W. Park, "Nonlinear parameter optimization of FACTS controller via real-time digital simulator," *IEEE Trans. Ind. Appl.*, vol. 49, no. 5, pp. 2271–2278, Sep./Oct. 2013.
[21] W. Qiao, G. K. Venayagamoorthy, and R. G. Harley, "Real-time implementation of a STATCOM on a wind farm equipped with doubly fed induction generators," *IEEE Trans. Ind. Appl.*, vol. 45, no. 1, pp. 98–107, Jan./Feb. 2009.
[22] H.-X. Li, "Adaptive fuzzy controllers based on variable universe," *Sci. China E, Technol. Sci.*, vol. 42, no. 1, pp. 10–20, Feb. 1999.
[23] H.-X. Li and C. L. P. Chen, "The equivalence between fuzzy logic systems and feedforward neural networks," *IEEE Trans. Neural Netw.*, vol. 11, no. 2, pp. 356–365, Mar. 2000.
[24] H.-X. Li, Z.-H. Miao, and E. S. Lee, "Variable universe stable adaptive fuzzy control of a nonlinear system," *Comput. Math. Appl.*, vol. 44, nos. 5–6, pp. 799–815, Sep. 2002.
[25] T. Logenthiran, D. Srinivasan, A. M. Khambadkone, and H. N. Aung, "Multiagent system for real-time operation of a microgrid in real-time digital simulator," *IEEE Trans. Smart Grid*, vol. 3, no. 2, pp. 925–933, Jun. 2012.
[26] W. Shan, Y. Ma, R. W. Newcomb, and D. Jin, "Analog circuit implementation of a variable universe adaptive fuzzy logic controller," *IEEE Trans. Circuits Syst., II, Exp. Briefs*, vol. 55, no. 10, pp. 976–980, Oct. 2008.
[27] D. Guha, P. K. Roy, and S. Banerjee, "Load frequency control of interconnected power system using grey wolf optimization," *Swarm Evol. Comput.*, vol. 27, pp. 97–115, Apr. 2016.
[28] C. Mu, Y. Tang, and H. He, "Improved sliding mode design for load frequency control of power system integrated an adaptive learning strategy," *IEEE Trans. Ind. Electron.*, vol. 64, no. 8, pp. 6742–6751, Aug. 2017.
[29] H. Bevrani and T. Hiyama, "On load–frequency regulation with time delays: Design and real-time implementation," *IEEE Trans. Energy Convers.*, vol. 24, no. 1, pp. 292–300, Mar. 2009.
[30] A. S. Wu, H. Yu, S. Jin, K.-C. Lin, and G. Schiavone, "An incremental genetic algorithm approach to multiprocessor scheduling," *IEEE Trans. Parallel Distrib. Syst.*, vol. 15, no. 9, pp. 824–834, Sep. 2004.
[31] N. Hou, F. He, Y. Zhou, Y. Chen, and X. Yan, "A parallel genetic algorithm with dispersion correction for HW/SW partitioning on multi-core CPU and many-core GPU," *IEEE Access*, vol. 6, pp. 883–898, 2017.
[32] Z. Wang, J. Li, K. Fan, W. Ma, and H. Lei, "Prediction method for low speed characteristics of compressor based on modified similarity theory with genetic algorithm," *IEEE Access*, vol. 6, pp. 36834–36839, 2018.
[33] F. Ma, L. Han, Y. Zhou, S. Chen, and Y. Pu, "Multi-island genetic algorithm and Kriging model-based design of vehicle product comprising multi-material," *IEEE Access*, vol. 6, pp. 53397–53408, 2018.
[34] K. P. Wong and Y. W. Wong, "Genetic and genetic/simulated-annealing approaches to economic dispatch," *IEE Proc.-Gener., Transmiss. Distrib.*, vol. 141, no. 5, pp. 507–513, Sep. 1994.
[35] M. E. C. Bento, D. Dotta, R. Kuiava, and R. A. Ramos, "A procedure to design fault-tolerant wide-area damping controllers," *IEEE Access*, vol. 6, pp. 23383–23405, 2018.
[36] *The Operation Mode of China Southern Power Grid in 2013*, (in Chinese), China Southern Power Grid Co., Guangzhou, China, 2013.
[37] H. Bevrani and T. Hiyama, *Intelligent Automatic Generation Control*. Boca Raton, FL, USA: CRC Press, 2011.
[38] Z. Gao, X. Teng, and T. Liqun, "Hierarchical AGC mode and CPS control strategy for interconnected power systems," (in Chinese), *Automat. Electr. Power Syst.*, vol. 28, no. 1, pp. 78–81, Jan. 2004.
[39] R. B. Chedid, S. H. Karaki, and C. El-Chamali, "Adaptive fuzzy control for wind-diesel weak power systems," *IEEE Trans. Energy Convers.*, vol. 15, no. 1, pp. 71–78, Mar. 2000.
[40] J. Talaq and F. Al-Basri, "Adaptive fuzzy gain scheduling for load frequency control," *IEEE Trans. Power Syst.*, vol. 14, no. 1, pp. 145–150, Feb. 1999.
[41] NERC. *Real Power Balancing Control Performance, BAL-001-1*. [Online]. Available: http://www.nerc.com/docs/standards/sar/Project2010-14-1BAL-001-1_Standard_Clean_20120604_final_rev1.pdf

SADDAM AZIZ (S'16) received the B.Eng. and M.Eng. degrees in electrical engineering from Chongqing University, Chongqing, China, in 2012 and 2015, respectively. He is currently pursuing the Ph.D. degree with the Department of Optoelectronic Engineering, Shenzhen University, Shenzhen, China. His research interests mainly include multi-terminal dc system operation, optimization, and planning.

HUAIZHI WANG (M'16) received the B.Eng. and M.Eng. degrees in control science and engineering from Shenzhen University, Shenzhen, China, in 2009 and 2012, respectively, and the Ph.D. degree in electrical engineering from the South China University of Technology, Guangzhou, China, in 2015. He was a Research Assistant with the Department of Electrical Engineering, Hong Kong Polytechnic University, Hong Kong, from 2014 to 2015. He is currently an Assistant Professor with Shenzhen University. His research interest includes automatic generation control in cyber physical power systems.

YITAO LIU (S'11–M'15) received the B.S. degree in electrical engineering from Wuhan University, Wuhan, China, in 2008, and the M.S. and Ph.D. degrees in electrical and electronic engineering from Nanyang Technological University (NTU), Singapore, in 2009 and 2014, respectively. From 2014 to 2015, he was a Research Fellow at the Rolls Royce-NTU Joint Laboratory. He is currently an Assistant Professor with Shenzhen University, Shenzhen, China. His current research interests include high power density converters, EMI/EMC in power electronics, and wideband-gap devices.

JIANCHUN PENG (M'04–SM'17) received the B.S. and M.S. degrees from Chongqing University, Chongqing, China, in 1986 and 1989, respectively, and the Ph.D. degree from Hunan University, Hunan, China, in 1998, all in electrical engineering. He was a Visiting Professor with Arizona State University, Tempe, AZ, USA, from 2002 to 2003, and with Brunel University, London, U.K., in 2006 He is currently a Professor with the College of Mechatronics and Control Engineering, Shenzhen University, Shenzhen, China. His current research interests include electricity markets, and power system optimal operation and control.

HUI JIANG received the B.S. degree from Chongqing University, Chongqing, China, in 1990, and the M.S. and Ph.D. degrees from Hunan University, Hunan, China, in 1999 and 2005, respectively, all in electrical engineering. From 2005 to 2006, she was a Visiting Scholar at Brunel University, London, U.K. She is currently a Professor with Shenzhen University. Her interests include power system economics, and power system planning and operation.